Comparison of Cameras: Dynamic Ranges and Sensitivities of optical CCDs.

Contact *lucy.wilson@stfc.ac.uk*

P. Oliver, A. Horn, R. J. Clarke, D. R. Rusby, G. Scott, L. A. Wilson, D. Neely

Central Laser Facility, STFC,
Rutherford Appleton Laboratory,
Oxon OX11 0QX, United Kingdom

Introduction

Cameras are used for collecting light and imaging in a wide range of diagnostics. The following report details properties and characteristic features of a range of different cameras used in experiments including charged coupled devices (CCD), electron multiplying charged coupled devices (EMCCD) and complementary metal–oxide–semiconductor (CMOS). The dynamic range and linearity of the cameras are compared and the different components of noise and their levels for each camera are studied. The cameras tested are listed in Table 1.

Dynamic Range and Linearity

The dynamic range quantifies the ability of a sensor to image a range of light intensities in the same image. It is defined as the ratio of the largest non-saturating input signal to the smallest detectable signal.[1] Saturation is when the pixels are exposed to so much light that the pixels cannot store more charge, meaning any additional signal is not recorded.

A 3x3cm green uniform light source was focused down onto the camera sensor using a 50mm diameter, 150mm focal length lens. The exposure time of the cameras was 100ms. The source was continuously on. The luminosity of the light source was uniform so that variance of the image across the source reflects non-uniformities in the camera.

A range of neutral density filters were placed in front of the light source in order to measure the linearity of the camera response to changes in light intensity.

Background images were taken with the light source on but with a very high level of filtering (to give a transmission of 0) to account for the signal scattered into the CCD from any leaks in the shielding as well as the dark current. The difference between the background and dark current readings (light source removed) was found to be on the order of a few counts so shielding was assumed to be adequate. This average background taken over 10 exposures was subtracted from the images taken during the linearity tests. The counts were measured across a region of the camera chip that was evenly illuminated with no defective pixels, the same area size was used on each camera.
For colour cameras the signal from the pixels with a green filter were separated out from the other colours as the light source was green. This was used for comparison to monochromatic cameras.

In figures 1 and 2, the graph of standard deviation and mean number of counts are plotted for different filter transmissions.

The SX-25C responds differently from the other cameras near saturation and has a less linear response. This is because the SX-25C camera has anti-blooming features. Blooming occurs when a pixel saturates causing excess charge to spill into adjacent pixels. The anti-blooming feature removes excess charge to prevent it spilling over into neighboring pixels [2], the onset of this is not linear and results in reduced sensitivity. The starlight express SX-694, SX-25C and H9C and the Andor neo have similar response with dynamic ranges of around 10^4. However, the neo appears to have the most linear response down towards the noise level. The Kite appears to have an additional source of background noise not removed by the background subtraction giving a dynamic range of around 10^3 - 10^2.

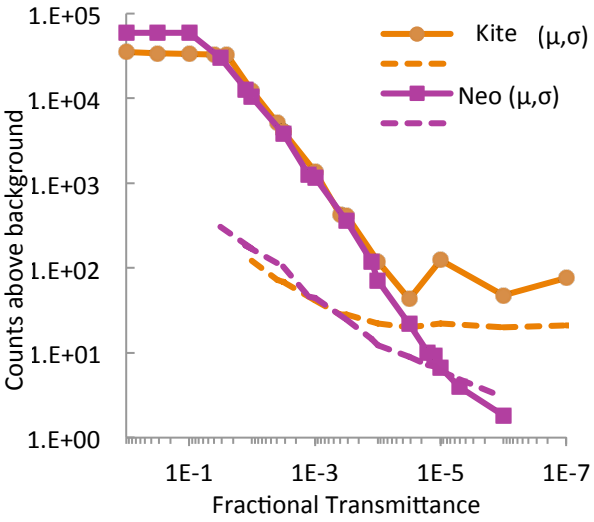

Figure 1: Linearity curve for Raptor kite EMCCD and Andor Neo CMOS cameras

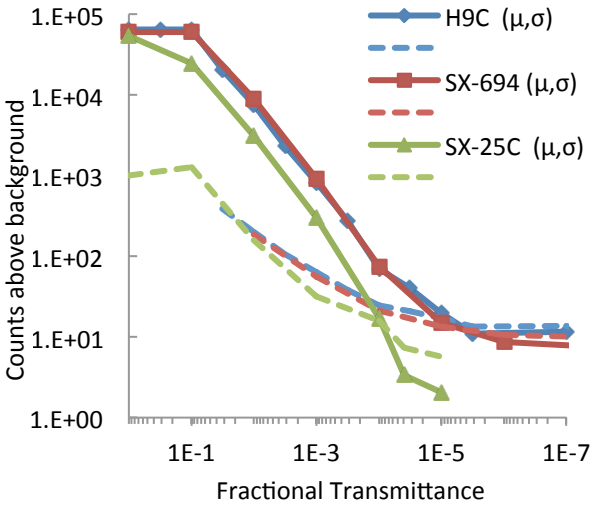

Figure 2: Linearity curve for SXVF-H9C, Trius SX-694 and Trius SX-25C CCDs.

Defective Pixels

Every camera tested is made up of over 200 000 pixels, even with a very low manufacturing defects, some pixels are expected to be defective. Only if a region or a significant percentage is defective does action need to be taken.

Hot pixels are caused due to the thermal generation of electron-hole pairs from damage caused by high energy cosmic rays or other processes. The dark current in these pixels is much higher

than in neighboring pixels [3,4]. These are a form of fixed pattern noise (FPN) so can be removed by subtracting a background image in post processing. To find defective pixels, the CCD is shielded from light using aluminum foil and many images are taken. The images are averaged and any pixels which have higher count rates than surrounding pixels are deemed as defective. Summarized results are listed in Table 2. The Starlight express cameras all have similar numbers of defective pixels (<20), the Raptor kite however has double this number with 40 defective pixels.

Readout Noise

Readout noise is a random Gaussian noise of the camera caused by the readout architecture. It cannot be reduced by background subtraction. It can be measured by exposing the camera for the shortest possible time so dark current can be assumed to be negligible, in light tight conditions (this is a bias image). In post processing, a large value is added to every pixel (to stop zeroing issues) then the average of the bias images is subtracted. The image which remains is the isolated readout noise, which should be a Gaussian noise. The fast-Fourier transform (FFT) of the image shows the distribution of frequencies in the image, any patterns in this image is a sign there is a periodic component to the readout noise. This cannot be removed by averaging a series of images and will shrink the dynamic range and the signal to noise ratio. The readout noise of each camera is listed in table 2. All the cameras tested where found to have similar levels of readout noise. None of the cameras showed significant periodic noise.

Dark Current and Temperature

Dark current only images were taken with the camera chip covered. Dark current is a signal caused by electrons absorbing thermal energy and crossing the band gap. It is proportional to the sensor material, pixel size, the exposure time and absolute temperature. Most cameras tested have internal thermoelectric coolers; some also have a thermometer so temperature can be measured. To test the cooling, the camera was cooled, shielded and fixed exposure time images (30s) were taken. An example of the change in dark current as a camera is cooled over a period of time is given in Figure 3, with the count rate clearly decreasing as the camera is cooled. Figure 4 shows the effect of increasing exposure time on dark current. To test the dark current, when the temperature had stabilized, images of increasing exposure time were taken. The time taken to cool to the maximum possible cooling is given with the counts per second of the dark current. The measured SX-694 and SXVF-H9C camera dark current is given in table 2 with the SXVF-H9C having a larger dark current this could be due to its larger pixels.

Conclusions

The dynamic range, linearity and noise levels of a variety of CMOS and CCD cameras have been measured. The starlight express SX-694, SX-25C and H9C and the Andor Neo were all found to have dynamic ranges of around 10^4. The Raptor Kite had a dynamic range of around 10^3 - 10^2 due to background noise. The cameras were all found to have similar amounts of readout noise, with the Raptor Kite having a larger number of defective pixels than the other cameras. Dark current was measured for the SX-694 and SXVF-H9C cameras. The SXVF-H9C was found to have a larger dark current most likely due to its larger pixels.

Acknowledgements

This work was supported through grant EP/K022415/1, Advanced laser-ion acceleration strategies towards next generation healthcare from EPSRC. The authors would like to thank the staff at the Central Laser Facility for their support. Data associated with research published in this paper can be accessed by contacting the corresponding author.

References

1. High Dynamic Range Image Sensors, *Abbas El Gamal* Department of Electrical Engineering, Stanford University, Lecture Slides, http://cafe.stanford.edu/~abbas/group/papers_and_pub/isscc02_tutorial.pdf
2. Andor.com, (2015). *CCD Blooming and Anti-blooming - The principle of blooming.* http://www.andor.com/learning-academy/ccd-blooming-and-anti-blooming-the-principle-of-blooming, Accessed 15 Sep. 2015.
3. Andor.com, (2015). CCD Blemishes and Non Uniformities - Black pixels and hot pixels on a CCD sensor. http://www.andor.com/learning-academy/ccd-blemishes-and-non-uniformities-black-pixels-and-hot-pixels-on-a-ccd-sensor Accessed 15 Sep. 2015.
4. "On Growing Better Decision Trees from Data", K. V. S. Murthy (2015). Hot Pixels. Available at: http://www.cbcb.umd.edu/~salzberg/docs/murthy_thesis/node65.html. Accessed 15 Sep. 2015.
5. Qsimaging.com, (2015). Understanding CCD Read Noise. http://qsimaging.com/ccd_noise.html. Accessed 15 Sep. 2015.

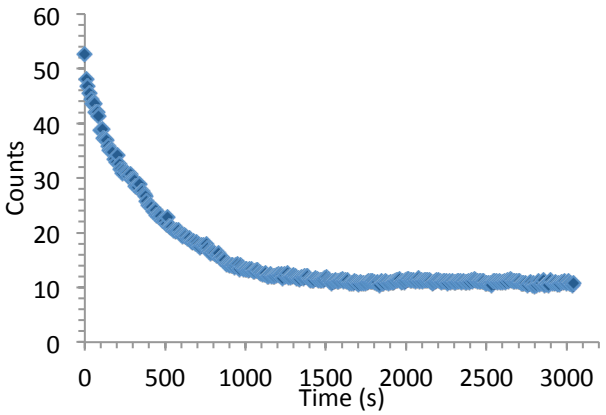

Figure 3: Dark current against time for a SX-25C CCD as it is cooled from room temperature to -15C over time.

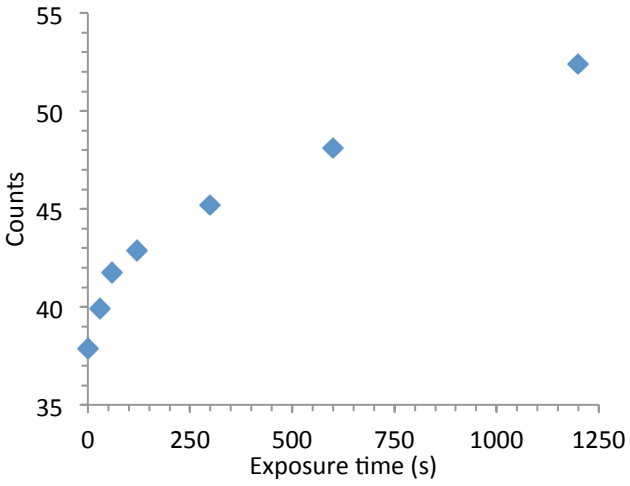

Figure 4: Dark current against exposure time for a SX-25C CCD.

Camera Name	Manufacturer	Active Pixels	Sensor Type	Pixel Size (μm)	Cooling
Trius SX-25C	Starlight Express	3032 x 2016	Colour CCD	7.4	-15°C held
Kite	Raptor Photonics	658x496	EMCCD	10	-20°C
Trius SX-694	Starlight Express	2750x2200	CCD	4.54	-15°C held
SXVF-H9C	Starlight Express	1392x1040	Colour CCD	6.45	No cooling
Neo 5.5	Andor	2560 x 2160	CMOS	6.5	-40°C

Table 1: List of cameras tested and their properties

Camera Name	Cooling Time	CCD Quality (# of Hot Pixels)	Readout Noise Measured (ADU)	Dark Current Measured (ADU/s)
Trius SX-25C	30±5 min	19±3	17	Not measured
Kite	20 seconds	40±15	17.8±0.05	Not measured
Trius SX-694	25±5 min	13±2	16±1	0.057±0.003
SXVF-H9C	40±10 min	15±2	17	0.082±0.002

Table 2: Noise data summary for tested cameras